69th International Astronautical Congress (IAC), Bremen, Germany, 1-5 October 2018.


IAC–18–A6.10-C1.7.8

# Evolution of Fragmentation Cloud in Highly Eccentric Earth Orbits through Continuum Modelling

**Stefan Frey[a*], Camilla Colombo[a], Stijn Lemmens[b]**

[a] *Department of Aerospace Science and Technology, Politecnico di Milano, Milan, Italy*
[b] *Space Debris Office, ESA/ESOC, Darmstadt, Germany*
[*] Corresponding author; stefan.frey@polimi.it

**Abstract**

A considerable number of fragments orbit around the Earth in Highly Eccentric Orbits (HEOs), mainly in the geostationary transfer orbit. These are believed to have originated in part from the 100 plus fragmentations of parent objects in the same orbit. Many of these objects are characterised by a high area-to-mass ratio, and, as such, especially susceptible to forces induced by atmospheric drag and solar radiation pressure. The complicated dynamics make it difficult to model the evolution of a cloud of such objects, as the spreading depends heavily on their area-to-mass ratios which is difficult to assess. Assumptions on the rapid distribution of a HEO fragment cloud into a band limited by its parent orbit inclination were shown to be inaccurate, and thus oversimplify the problem at hand. Moreover, the time to form a uniformly distributed cloud is higher than the time it takes many of the particles to re-enter.

This work aims to increase the understanding of these complex dynamics by accurately modelling the evolution of a cloud of fragments in HEO. The fragment cloud is modelled as a continuum, and its phase space density, rather than single objects, is propagated in time using averaged dynamics in Keplerian elements. Such an approach is not only much faster in terms of computational load when compared to the individual propagation of fragments, but it also improves the accuracy of the density estimation. The perturbations considered are atmospheric drag using a model that was specifically developed for highly eccentric orbits, solar radiation pressure, third bodies and a non-spherical central body implemented in the *PlanODyn* suite.
**Keywords: Space Debris, Continuum Modelling, Eccentric Orbit**

**Abbreviations**

| | |
|---|---|
| DISCOS | Database and Information System Characterising Objects in Space. |
| ESA | European Space Agency. |
| GTO | Geostationary Transfer Orbit. |
| HAMR | High Area-to-Mass Ratio. |
| HEO | Highly Eccentric Orbit. |
| LEO | Low Earth Orbit. |
| MC | Monte Carlo. |
| MCMC | Markov Chain Monte Carlo. |
| NASA | National Aeronautics and Space Administration. |
| PDF | Probability Distribution Function. |
| PlanODyn | Planetary Orbital Dynamics. |

## 1. Introduction

Out of the nearly 12500 space debris fragments which are orbiting Earth and being tracked on a regular basis, roughly 600 are located in the Geostationary Transfer Orbit (GTO), and hundreds more reside in other Highly Eccentric Orbits (HEOs) [1]. Objects in such orbits are generally difficult to observe as their apparent angular velocity, as well as their altitudes, vary over a wide range along their trajectories, meaning that the true number of objects in HEO might be underestimated [2]. Two decades ago, the European Space Agency (ESA) established an optical survey program to observe fragments at high altitudes, revealing a population of High Area-to-Mass Ratio (HAMR) objects, of unknown origin [3, 4]. Such objects are especially susceptible to solar radiation pressure, increasing and decreasing their inclination and eccentricity, potentially reducing the perigee sufficiently to be captured by the atmosphere. Unknown shape and attitude further complicate the orbit evolution of HAMR objects in HEO. Even now, the majority of the fragments in such orbits are of unknown origin despite knowledge of more than 100 fragmentations in orbits with high eccentricities ($\geq$ 0.2), according to the Database and Information System Characterising Objects in Space (DISCOS) [5].

In spite of their low mass, they can still constitute a danger for missions in Low Earth Orbit (LEO) due

to their high orbital velocities of 11 km/s at perigee. It is therefore of interest how a fragmentation in HEO affects other space missions in terms of collision risk. Long-term space debris evolutionary models such as DELTA [6] and LEGEND [7] can model fragmentations using representative objects. However, they rely on random selection of the fragments, which can result in very different collision risk estimations for each Monte Carlo (MC) simulation run.

A more insightful approach into the evolution of a cloud of fragments is by treating it as a continuum. McInnes [8] derived, based on the continuity equation, an analytical model for the evolution of space debris as a function of altitude. Letizia et al. [9] extended the approach to account for low eccentricities and applied it to model the evolution of a fragment cloud. But it was still limited to a simplified drag model and assumed randomisation of the particles into a band. For clouds in HEO, it can take decades for a band to form [10], limiting the application of the model using simplified dynamics.

In this work, the characteristics of the continuity equation are propagated semi-analytically, which allows the accommodation of more elaborate force models, and can be extended to any dimension. Similarly, Halder and Bhattacharya [11] applied this method for the dispersion analysis of satellite planetary entry. Here, the initial density distribution is sampled to find initial conditions for the characteristics, which are subsequently propagated. The densities are then interpolated to estimate the distribution in between characteristics, allowing further reductions in the number of required propagations.

Another method of integrating a phase space density numerically is through differential algebra, shown by Wittig et al. [12]. The advantage of the latter is that no interpolation is required in the neighbourhood of each grid point, as the Taylor expansion of the flow is propagated. However, the resulting accuracy is difficult to gauge as it depends on the propagation time and the truncation order of the approximating polynomial. Contrary to their approach, here a fully analytical formulation of the Jacobian is used, making the density propagation along each characteristic accurate down to the tolerances set during integration.

The paper is organised as follows; in Section 2 the formulation of the problem is discussed, in Section 3, the interpolation of the distribution is explained, Sections 4 and 5 describe the workflow and a casestudy of a fragmentation in a Molniya type orbit. Finally the conclusion and future work can be found in Section 6.

## 2. Density Modelling

The aim of this work is to find a fast and accurate way of predicting the evolution of a break-up on-orbit with hundreds of thousands of fragments, where individual propagation becomes infeasible. This section illustrates the advantages of density modelling compared to MC simulations and shows the formulation of the former.

### *2.1 Motivation*

In MC simulations, once the samples are drawn from a density or Probability Distribution Function (PDF) (used interchangeably in this paper), they become equi-probable. For a known distribution, such as a multi-variate Gaussian, it might be sufficient to fit the samples to the distribution. But as the dynamics start to distort the distribution over time, an analytical model cannot be fit and the density needs to be inferred for each point in the domain, e.g. by binning and counting the population. A large amount of equi-probable samples is required to accurately estimate the underlying distribution. This does not scale well with increasing dimensions, $d$, and decreasing bin sizes.

If instead the density itself is propagated forward in time, the evolving PDF at each point is directly and accurately given (only integration rounding errors need to be accounted for) and need not be estimated. Such a weighted approach reduces the number of required samples drastically, decreasing the computational load whilst still allowing estimation of the underlying PDF with enough accuracy (see Section 3).

### *2.2 Formulation*

The model is based on the differential form of the general continuity equation [8]

$$\frac{\partial n}{\partial t} + \nabla \cdot (n\boldsymbol{F}) = 0 \tag{1a}$$

$$\frac{\mathrm{d}\boldsymbol{x}}{\mathrm{d}t} = \boldsymbol{F} \tag{1b}$$

with the density, $n \in \mathbb{R}$, the independent variable time, $t \in \mathbb{R}$, the phase space, $\boldsymbol{x} \in \mathbb{R}^d$, and the dynamics, $\boldsymbol{F} \in \mathbb{R}^d$, and ignoring sources and sinks. The partial differential equation 1 can be turned into the following ordinary differential equation, using the method of the characteristics (following the derivations of [9], with slightly different notation)

$$\frac{\mathrm{d}n}{\mathrm{d}t} + n\sum_{i=1}^{d}\frac{\partial F_d}{\partial x_d} = 0 \tag{2a}$$

$$\frac{\mathrm{d}\boldsymbol{x}}{\mathrm{d}t} = \boldsymbol{F} \tag{2b}$$

As is evident in the extended phase space, $\boldsymbol{x}^* = [\boldsymbol{x}, n]$, the characteristics of the system in Equation 1 simply follow the trajectories of the dynamics and the density changes exponentially with the negative trace of the Jacobian of the dynamics. This is convenient, as it allows for the comparison of the traditional MC and the density approach using the same sample population.

## 3. Continuum Estimation

Given the population of samples at any time after the fragmentation, $\Delta t_i$, the full PDF in the domain of interest, e.g. the domain affecting a certain orbital region, needs to be estimated.

### *3.1 Methods*

In a case where the samples are all equi-probable, the bin count just needs to be multiplied by the fixed weight. In case the information of the density – a variable weight – is available, there are two different ways to infer the distribution; either through averaging over the weighted samples within each bin; or through interpolating between the weighted samples. Figure 1 illustrates the three different ways of estimating the density from 500 samples in $\mathbb{R}^2$. The averaging, while very simple and fast, requires at least one sample to be in each bin, or else the bin is assumed to have zero density. With too small bin sizes or an insufficient number of samples, the total number of fragments will thus be underestimated. The interpolation, on the other hand, can deal with ever smaller bins or diverging dynamics. However, its complexity increases with non-convex, or highly localised distributions. Both methods tend to overestimate the total number of objects if the bin sizes are too large.

### *3.2 Interpolation Procedure*

The interpolation is performed on a grid using Delaunay triangulation between the samples to find the $d$-simplexes. Subsequent linear interpolation uses the barycenter coordinates of each simplex together with the weights of the vertices [13]. For interpolation points outside of any simplex, the density is set to zero. Integration over the bins computes the total number of fragments, $N_f$. If the distribution is well behaved, i.e. convex and non-localised, this is already sufficient.

However, in most cases, the distribution of a cloud of fragments tends to be non-convex. One way of handling such cases is resorting to $\alpha$-shapes, which can more accurately capture the true shape of a distribution in any dimension [14]. Instead here, a simple control variable, $\beta$, is introduced to remove all simplexes where the maximum distance in between any of the corresponding samples is larger than $\beta$. This control parameter can be optimised such that $N_f$ matches the one added up through the equi-probable method. Since $N_f \in \mathbb{R}$ is a single dimensional quantity, it can be recovered very accurately from the latter. Clearly, this is only a first solution of the problem of non-convex shapes, with room for improvement in future work.

Another problem is that the chosen interpolation points, here a grid for easy subsequent integration, can miss large parts of the distribution if it is highly localised, i.e. is nearly non-spread in at least one dimension. Decreasing the bin size helps, but for increasing $d$ will very quickly lead to memory issues. One solution would be to use an adaptive density mesh, which could be readily derived from the simplexes given from the triangulation. Integrating each simplex would result in higher accuracy, without the need for large memory. The example shown in Section 5 is only in $\mathbb{R}^3$ and sufficiently spread, but for extensions into higher dimensions, more work is required.

## 4. Tools

Figure 2 shows a schema of the steps involved. First, the cloud distribution needs to be drawn, which is generally modelled independently of the fragmentation location on the orbit. Together with the parent orbit, the phase space selection and the binning, the fragment cloud defines the initial continuum. From there, initial characteristics are drawn, which are then propagated from the initial to the final time with given step sizes, $\Delta t_0, \Delta t_1, \ldots, \Delta t_f$. After grouping the characteristics, the continuum can be retrieved for each time step, $\Delta t_i$.

### *4.1 Fragment Distribution & Initial Continuum*

Any break-up model that gives the distribution in orbital elements and fragment characteristics can be used. Herein, the National Aeronautics and Space Administration (NASA) break-up model [15] is employed, which gives the fragment properties in terms of characteristic length, area-to-mass ratio, $A/m$, and the initial velocity impulse, $\Delta v$. The direction in which $\Delta v$ is introduced needs to be drawn randomly.

Together with the information of the parent orbit and fragmentation location, initial fragment orbits can be determined. The distribution is transformed into Keplerian states by sampling.

### *4.2 Initial Characteristic Selection*

Theoretically, the evolution of the distribution is not dependent on the initial selection of characteristics. To keep the number of characteristics, $N_c$, low,

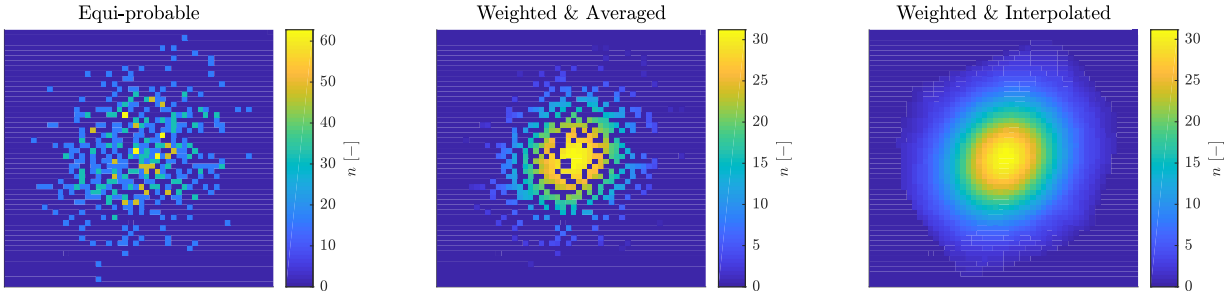


(a) From equi-probable samples, resulting in a very poor estimation.

(b) From weighted samples using the average method, resulting in an accurate estimation, albeit full of holes.

(c) From weighted samples using the interpolation method, resulting in a very accurate estimation for this simple convex distribution.

Fig. 1: Estimation of the underlying distribution from a population of 500 samples using different methods. The colour code shows the density, i.e. number of fragments divided by bin area.

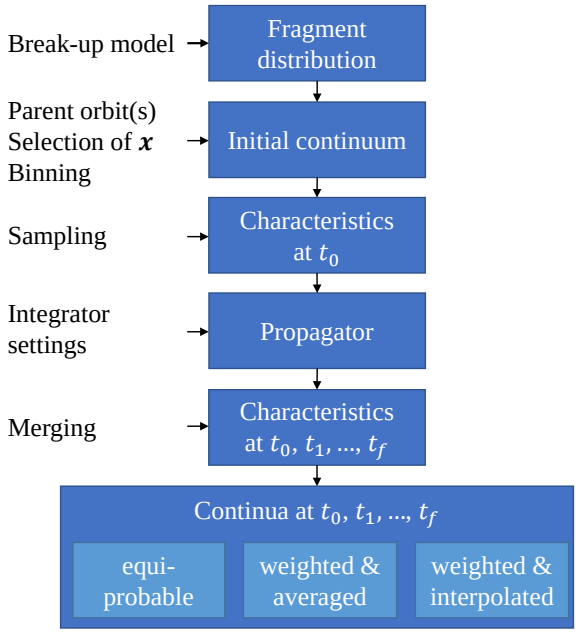


Fig. 2: Schema of the steps involved for estimating the density at different time steps, given a break-up scenario.

they should contain as much information of the initial distribution as possible. E.g. points with zero probability are not of interest, as – without sources – the density along those characteristics remains zero (see Equation 2a). Instead, they are sampled from the initial continuum using a Markov Chain Monte Carlo (MCMC) method, e.g. regions of high probability are represented with more characteristics. Here, the Metropolis-Hastings algorithm [16] is used in normalised space as the variables in $\boldsymbol{x}$ are generally of different units.

### *4.3 Propagation*

The trajectories are integrated using the Planetary Orbital Dynamics (PlanODyn) suite [17], a semi-analytical propagator. The suite analytically calculates the Jacobian of the dynamics required for the integration of $n$. The gravitational perturbations taken into account are due to the second degree zonal harmonic, $J_2$, as well as due to the moon and Sun gravity, whose positions were taken from NASA's Spice toolkit [18]. Solar radiation pressure was considered using the Cannonball model. Orbital decay due to atmospheric drag was estimated using a superimposed exponential fit to the Jacchia-77 atmospheric density model (with fixed exospheric temperature, $T_\infty = 1000$ K), and computed using an extended King-Hele orbital contraction model [19, 20].

### *4.4 Interpolation*

Lastly, the *equi-probable*, *weighted & averaged* and *weighted & interpolated* continua are derived from the same population of fragments using the methods described in Section 3.

Table 1: Parent orbit as of 12pm, 9 September, 1981, given in semi-major axis, $a$, eccentricity, $e$, inclination, $i$, right ascension of the ascending node, $\Omega$, and the argument of perigee, $\omega$.

| $a$ [km] | $e$ [−] | $i$ [deg] | $\Omega$ [deg] | $\omega$ [deg] |
|---|---|---|---|---|
| 13577 | 0.4537 | 63.4 | 300.9 | 330.6 |

## 5. Case Study

The studied case is inspired by the real fragmentation of a rocket body with international identifier 1981-088F, which unsuccessfully attempted to deliver a communications satellite into a Molniya type orbit, but malfunctioned during the orbit raise burn shortly after launch [21].

### *5.1 Fragmentation Type*

Fragments down to 1 mm are considered, resulting in $N_f = 360000$ objects, according to the break-up model assuming a rocket body explosion with scaling factor, $S = 1$.

### *5.2 Parent Orbit*

The epoch and orbital elements are taken from DISCOS and listed in Table 1. Due to a lack of better information, the location of fragmentation is assumed to be at the right ascension of ascending node, $\Omega$, i.e. at a mean anomaly of $M_f = 10.1$ deg. The parent orbit sits on the critical inclination, which cancels out the drift of the argument of perigee, $\omega$. So fragments with small inclination changes in positive and negative directions are expected to drift apart in $\omega$. Due to the high perigee and apogee altitudes of $1038 \times 13359$ km, the fragments will initially mainly be influenced by solar radiation pressure and the third bodies. Eccentricity build-up and the large surface area will lead to atmospheric re-entry at a later stage.

### *5.3 Phase Space*

In a first approximation of the evolving distribution, the phase space is chosen to be $\boldsymbol{x} = (a, e, A/m) \in \mathbb{R}^3$, where $a$ and $e$ are the semi-major axis and eccentricity respectively. This is a trade-off between balancing accuracy and the computational memory at hand (see Section 3). The characteristics still contain information about the evolution in inclination, $i$, $\Omega$ and $\omega$. To simulate the initial condition outside of $\boldsymbol{x}$, $i$, $\Omega$ and $\omega$ are drawn individually from a Gaussian distribution, as expected according to the break-up model, with standard deviations, $\sigma_i/\sigma_\Omega/\sigma_\omega = 0.5/0.0/0.025$ deg. Note that the distribution in $\Omega$ is zero, as the fragmentation is modelled to occur at the node.

Table 2: Root mean square of the differences in the density estimation against the original density over all the bins. The errors are given in $[\mathrm{km}^{-1}(\mathrm{m}^2/\mathrm{kg})^{-1}]$.

| Estimation method | Number of characteristics, $N_c$ $10^3$ | $10^4$ | $10^5$ |
|---|---|---|---|
| equi-probable | $1.8 \times 10^4$ | $6.1 \times 10^3$ | $2.5 \times 10^3$ |
| averaged | $5.8 \times 10^3$ | $3.5 \times 10^3$ | $2.2 \times 10^3$ |
| interpolated | $2.7 \times 10^3$ | $1.9 \times 10^3$ | $1.1 \times 10^3$ |

### *5.4 Accuracy on Inferring Initial Continuum*

The different methods of inferring the PDF from the samples are compared against the initial continuum, which is illustrated in Figure 3 for 100 bins in each dimension, linearly spaced in $a$ and $e$ and logarithmically spaced in $A/m$. The root mean square of the differences in estimated and true density over all the bins can be found in Table 2 for different $N_c$. The results depend on the method of interpolation of the initial weights, for which here a linear grid interpolation method was chosen, but a similar trend can be observed also for other methods. As expected, the weighted approach outperforms the equi-probable summation and the interpolation manages to fill the gaps caused by empty bins. The larger the number of characteristics, the better the estimation for all the methods.

### *5.5 Evolution*

The cloud was propagated for 100 years to see the long term effects on the density, depicted in Figure 4 for $\Delta t = 0$, 50 and 100 years after fragmentation. Only the integration over $A/m$ ratio is shown, as the area of the target satellite or rocket body generally is much larger than the fragment itself. Initially, the optimised $\beta$-value, a measure for the simplex sizes, is rather high ($\beta > 2$ in normalised space), as the cloud is still very compact, then, as the sample population starts to diverge, it reduces to a near constant $\beta = 0.16$. It is not useful at this point to compare the evolution estimated from $N_c = 1000$ characteristics using the interpolated method against the one estimated from $N_c = 100000$ characteristics using the equi-probable method, because, as can be seen from Table 2, the errors for both scenarios are in the same order of magnitude. Hence, for a fair assessment of the interpolation method, the fragment population needs to be increased even further to improve the accuracy of the equi-probable method. Future work will deal with this using an analytical formulation of

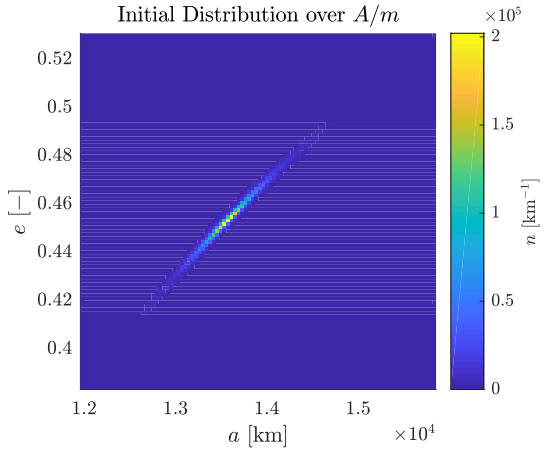


(a) Integrated over $A/m$.

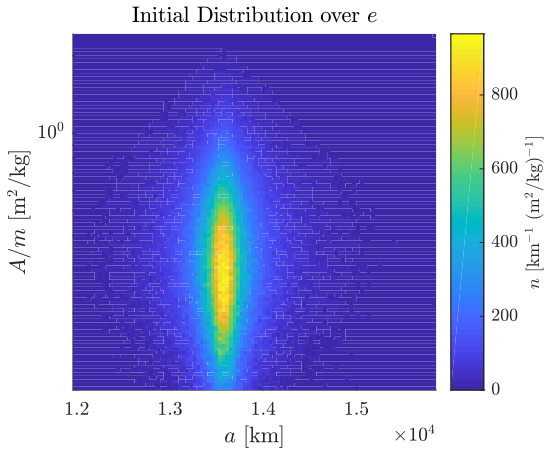


(b) Integrated over $e$.

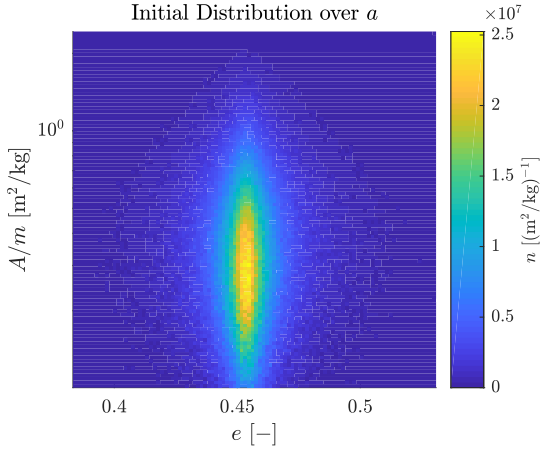


(c) Integrated over $a$.

Fig. 3: Initial distribution of a HEO rocket body fragmentation in $a$, $e$ and $A/m$.

the third body ephemerides, the current bottleneck of the propagation.

## 6. Conclusion and Future Work

The evolution of a cloud of space debris is modelled through interpolation of the characteristics of the continuum equation, where each sample caries the information of the distribution along the trajectory. This approach allows us the modelling of any degree of complexity in the dynamics. It was shown to estimate the underlying distribution function much more accurately than inference through equi-probable samples, allowing a reduction in the number of samples required to propagate. A low number of samples also means a small amount of disk space required to share the information with interested parties.

The problems identified with the interpolation are two-fold; first the proper identification of voids is required so as not to integrate over a volume of zero probability and hence overestimate the number of fragments. The second problem is related to the points of interpolation. If the interpolation grid is chosen to be too large, highly localised distributions might be missed and not accounted for. Simply decreasing the grid size, however, will exceed available memory capacity, especially for $d \geq 4$.

Once these issues are addressed, the phase space will be extended to also include $i$, $\Omega$ and $\omega$, expanding the applicability of the method to any fragmentation, and even the whole space debris population. Finally, given a smart way of converting the phase space density into a spatial density, the method could be applied to give accurate information about collision risk in a statistically coherent way without resorting to MC simulation.

## Acknowledgement

This project has received funding from the European Research Council (ERC) under the European Union's Horizon 2020 research and innovation programme (grant agreement No 679086 - COMPASS).

## References

[1] ESA's Space Debris Office. ESAs annual space environment report, produced with the discos database, 2018.

[2] T. Schildknecht, R. Musci, M. Ploner, G. Beutler, W. Flury, J. Kuusela, J. de Leon Cruz, and L. de Fatima Dominguez Palmero. Optical observations of space debris in GEO and in highly-eccentric orbits. *Advances in Space Research*, (34):901–911, 2004.

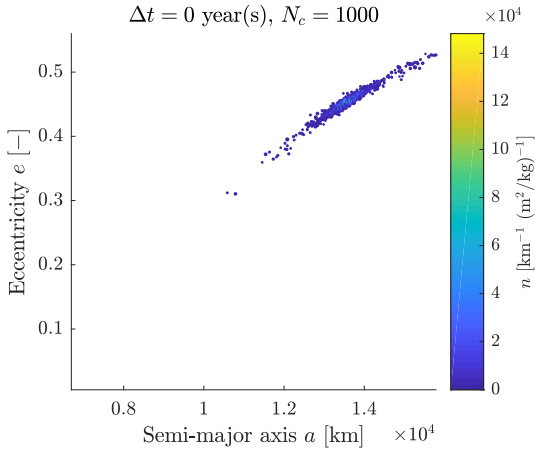


(a) Characteristics at $\Delta t = 0$ years.

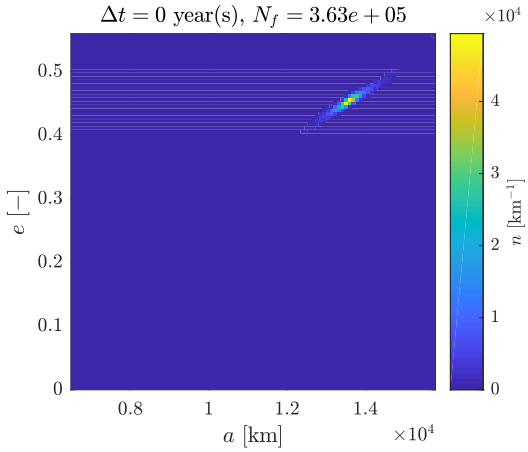


(b) Estimated density at $\Delta t = 0$ years.

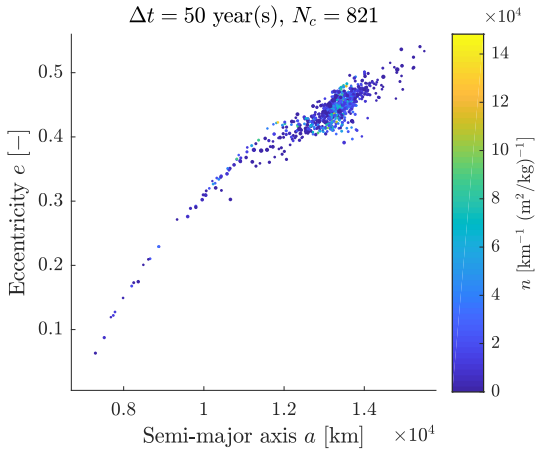


(c) Characteristics at $\Delta t = 50$ years.

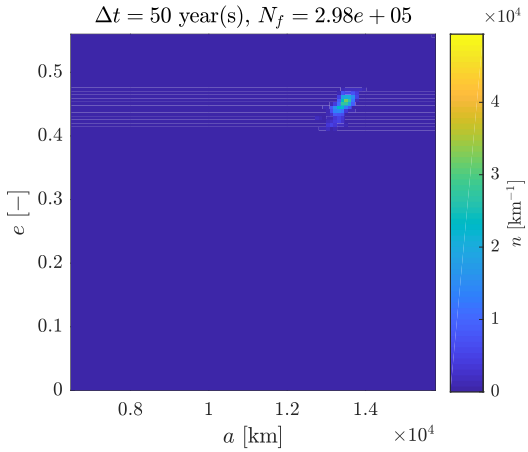


(d) Estimated density at $\Delta t = 50$ years.

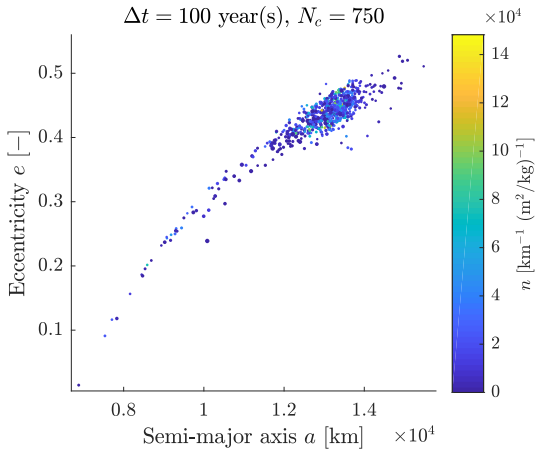


(e) Characteristics at $\Delta t = 100$ years.

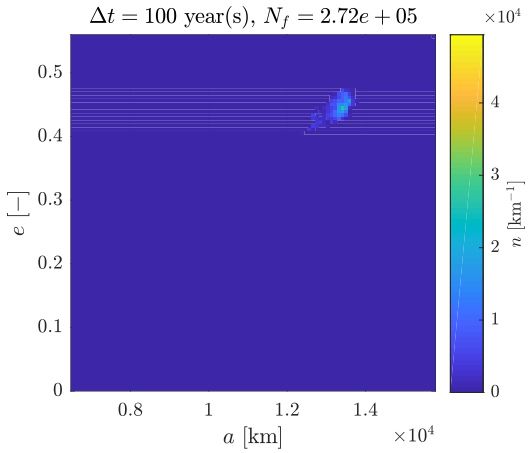


(f) Estimated density at $\Delta t = 100$ years.

Fig. 4: Characteristics and estimated density through the interpolation method, integrated over $A/m$ for different time steps. The size and color of the characteristics correspond to $A/m$ and $n$ respectively.

[3] J.-C. Liou and J. K. Weaver. Orbital dynamics of high area-to-mass ratio debris and their distribution in the geosynchronous region. In *In Proceedings of the 4nd European Conference on Space Debris*, 2005.

[4] T. Schildknecht, R. Musci, and F. Flohrer. Properties of the high area-to-mass ratio space debris population at high altitudes. *Advances in Space Research*, (41):1039–1045, 2008.

[5] F. McLean, S. Lemmens, Q. Funke, and V. Braun. DISCOS 3: An improved data model for ESA's database and information system characterising objects in space. In *Proceedings of the 7th European Conference on Space Debris*, 2017.

[6] B. Bastida Virgili. DELTA debris environment long-term analysis. In *Proceedings of the 6th International Conference on Astrodynamics Tools and Techniques (ICATT)*, 2016.

[7] J.-C. Liou, D. T. Hall, P. H. Krisko, and J. N. Opiela. LEGEND - a three-dimensional LEO-to-GEO debris evolutionary model. *Advances in Space Research*, 34(5):981–986, 2004.

[8] C. R. McInnes. An analytical model for the catastrophic production of orbital debris. *ESA Journal*, 17:293–305, 1993.

[9] F. Letizia, C. Colombo, and H. G. Lewis. Multi-dimensional extension of the continuity equation method for debris clouds evolution. *Advances in Space Research*, 57:1624–1640, 2016.

[10] S. Frey, C. Colombo, S. Lemmens, and H. Krag. Evolution of fragmentation cloud in highly eccentric orbit using representative objects. In *Proceedings of the 68th International Astronautical Congress*, 2017.

[11] A. Halder and R. Bhattacharya. Dispersion analysis in hypersonic flight during planetary entry using stochastic liouville equation. *Journal of Guidance, Control, and Dynamics*, 34(2):459–474, 2011.

[12] A. Wittig, C. Colombo, and R. Armellin. Long-term density evolution through semi-analytical and differential algebra techniques. *Celestial Mechanics and Dynamical Astronomy*, 128:435–452, 2017.

[13] D. F. Watson. *Contouring: A guide to the analysis and display of spatial data*. Pergamon, 1994.

[14] H. Edelsbrunner, D. G. Kirkpatrick, and R. Seidel. On the shape of a set of points in the plane. *IEEE Transactions on Information Theory*, IT-29(4):551–559, 1983.

[15] N. L. Johnson, P. H. Krisko, J.-C. Liou, and P. D. Anz-Maedor. NASA's new breakup model of EVOLVE 4.0. *Advances in Space Research*, 28(9):1377–1384, 2001.

[16] S. Chib and E. Greenberg. Understanding the metropolis-hastings algorithm. *The American Statistician*, 49(4):327–335, 1995.

[17] C. Colombo. Planetary orbital dynamics (PlanODyn) suite for long term propagation in perturbed environment. In *Proceedings of the 6th International Conference on Astrodynamics Tools and Techniques (ICATT)*, 2016.

[18] C.H. Acton. Ancillary data services of NASA's navigation and ancillary information facility. *Planetary and Space Science*, 44(1):65–70, 1996.

[19] L. G. Jacchia. Thermospheric temperature, density, and composition: new models. *SAO Special Report*, 375, 1977.

[20] D. King-Hele. *Theory of satellite orbits in an atmosphere*. London Butterworths, 1964.

[21] NASA's Orbital Debris Program Office. History of on-orbit satellite fragmentations, 14th edition, 2008.